Adenoviral vector-mediated rescue of the OMP-null phenotype *in vivo*

Lidija Ivic[1], Martina M. Pyrski[2], Joyce W. Margolis[2], Linda J. Richards[2], Stuart Firestein[1] and Frank L. Margolis[2]

[1] *Department of Biological Sciences, 923 Fairchild, MC 2438, Columbia University, New York, New York 10027, USA*

[2] *Department of Anatomy and Neurobiology, University of Maryland, School of Medicine, HSF 280, 685 West Baltimore Street, Baltimore, Maryland 21201, USA*

Correspondence should be addressed to S.F. (sjf24@columbia.edu)

The use of gene deletion by homologous recombination to determine gene or protein function has wide application in vertebrate neurobiology. An ideal complement to gene deletion would be subsequent gene replacement to demonstrate re-acquisition of function. Here we used an adenoviral vector to replace the olfactory marker protein (OMP) gene in olfactory receptor neurons of adult OMP-null mice and demonstrated the subsequent re-acquisition of function. Our results show that short-term expression of OMP restores the kinetics of electrophysiological responses of OMP-null mice to those of the control phenotype. This adenoviral-mediated rescue of the OMP-null phenotype is consistent with involvement of OMP in olfactory transduction.

Olfactory marker protein (OMP) is a small (19 kDa) cytosolic protein expressed at high levels by mature olfactory neurons in virtually all vertebrate species[1–4]. The OMP gene has been cloned[5], and the generation of OMP-null mice[6] provides insight into the gene's function. Electrophysiological recordings show that olfactory neurons in OMP-null mice have a reduced ability to respond to odor stimuli[6]. This altered physiological ability is reflected in slower onset and offset rates and in a slower recovery from adaptation. In addition, OMP-null mice have a higher detection threshold as monitored in behavioral assays[7]; they require 50–100 fold higher concentrations of odorant to reach a standard response.

These effects suggest that OMP is directly involved as a modulator in the olfactory signal transduction pathway. Alternatively, these results could be indirectly caused by anatomical or metabolic changes in olfactory receptor neurons (ORNs). Such changes could affect the survival and viability of ORNs, as OMP is reported to have mitogenic activity *in vitro*[8]. These two interpretations could be distinguished by replacing the gene for OMP in the adult OMP-null mouse and determining whether normal cellular responses to odorant stimuli are restored. If function is not restored, or is significantly delayed, this would support a developmental or structural involvement of OMP, which indirectly affects signaling. If restoration of function occurs rapidly, then this would indicate that OMP is directly involved in the odorant signaling cascade.

Replication-deficient recombinant adenovirus[9] is used as a tool to efficiently infect various mammalian host cells. In the peripheral olfactory system, adenovirus selectively infects mature olfactory neurons in adult rats[10] and mice[11] *in vivo*. Recombinant adenoviral vectors direct the functional expression of olfactory receptor genes in rat and mouse olfactory neurons[12,13]. To restore the function of the olfactory marker protein (OMP) in OMP-null mice and to analyze its potential role in the olfactory signal transduction pathway, we generated an adenoviral vector carrying the OMP gene. This vector was used to drive short-term (acute) expression of OMP in olfactory sensory neurons of control and OMP-null mice. Electrophysiological recordings done 1–4 days after viral infection showed rescue of the null phenotype, suggesting a direct role for OMP in the signal transduction pathway. This shows that a viral vector can be used in the olfactory neuroepithelium of a living mouse to restore and confirm the function of a deleted gene.

Results

Generation of CMV-OMP-IRES-EGFP adenovirus

We generated an E1-substituted recombinant adenovirus CMV-OMP-IRES-EGFP-AdV that carries the coding regions for the olfactory marker protein (OMP) and the enhanced green fluorescent protein (EGFP) linked by an internal ribosome entry site (IRES). In this construct, transcription was initiated by the cytomegalovirus promoter (CMV), and translation of the bicistronic transcript yielded OMP and EGFP as two separate proteins. Co-expression of OMP and GFP was detected in infected HEK 293 cells and olfactory neurons as early as 30 hours after infection. This was demonstrated by immunohistochemistry for OMP and by fluorescence microscopy for GFP.

The efficacy of the CMV-OMP-IRES-EGFP-AdV was evaluated *in vitro* and *in vivo* by both direct fluorescence and immunoblot analysis. Protein expression was initially evaluated in HEK 293 cells after infection with the recombinant adenovirus. The intense green fluorescence in the HEK 293 monolayer demonstrated viral infection and EGFP expression (data not shown); immunoblot analysis of extracts from these infected HEK 293 cells demonstrated co-expression of native OMP of the correct molecular weight (**Fig. 1a**). To test the efficacy of the recombinant virus *in vivo*, we infected the olfactory epithelium of OMP-null mice by intranasal irrigation. The extent and duration of contact of the viral solution with the olfactory epithelium was affected by several factors, including the position of the mouse during infection, inter-animal variability in nasal anatomy and rates of mucus flow and respiration. The co-expression of

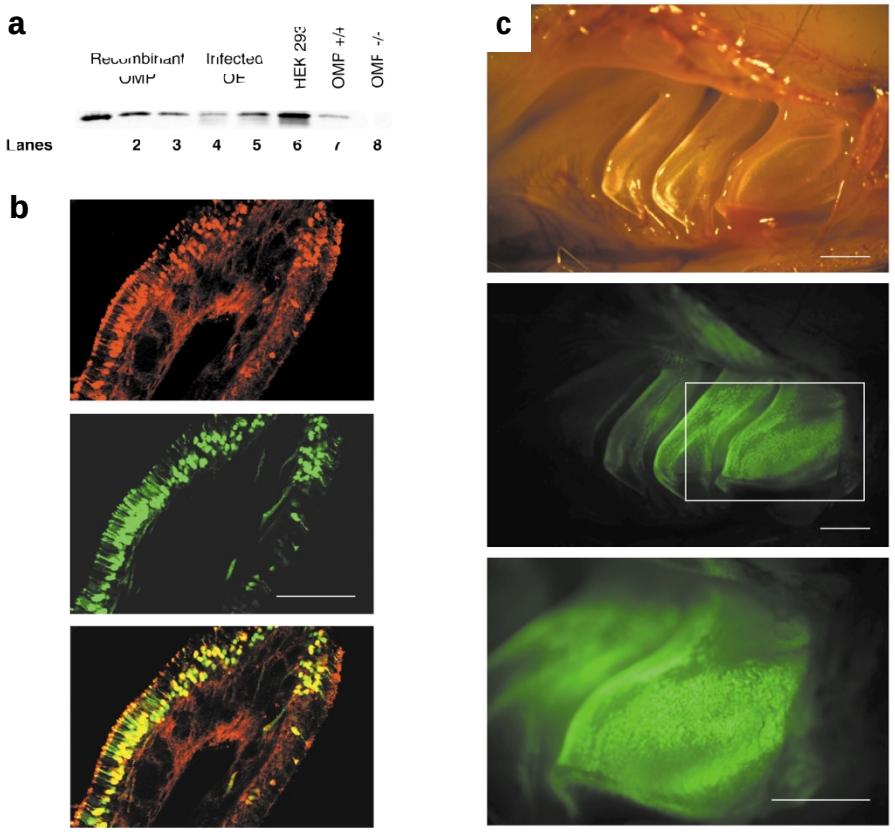

Fig. 1. Cells infected with the recombinant CMV-OMP-IRES-EGFP-AdV expressed both OMP and EGFP. (**a**) Western blot analysis of OMP expression. Lanes 1, 2 and 3, recombinant OMP: 1.5 μg, 1.0 μg and 0.5 μg, respectively. Lanes 4 and 5, 25 μg of protein extract from CMV-OMP-IRES-EGFP-AdV-infected nasal septum estimated to represent 20% and 40–50% infection, respectively. Lane 6, 20 μg of extract protein from CMV-OMP-IRES-EGFP-AdV-infected HEK 293 cells. Lanes 7 and 8, 40 μg of cytoplasmic extract protein from olfactory epithelium of 129 SvIm/J control and OMP-null mice, respectively. The electrophoretic mobilities of native and recombinant OMP were identical in all lanes. The intensities of lanes 4 and 5 bracketed that of lane 7 (control mouse), indicating that the level of OMP expression after AdV infection was at or above the control level. (**b**) Co-expression of OMP and GFP in olfactory neurons of OMP-null mice. The confocal fluorescence photograph of a coronal cryosection (12 μm) through the olfactory epithelium of OMP-null mice 4 days after infection (CMV-OMP-IRES-EGFP-AdV) demonstrated that OMP (red) and GFP (green) were colocalized. The section was taken from a ventral turbinate in the more caudal region. Olfactory neurons were identified by their typical morphology. Overlay of the two confocal images demonstrated colocalization (yellow) of GFP and OMP expression. Scale bar, 100 μm. (**c**) Whole-mount view of the olfactory epithelium in CMV-OMP-IRES-EGFP-AdV-infected OMP-null mouse (brightfield, top; fluorescence, middle and bottom). GFP expression (middle and bottom, bottom enlarged from the middle micrograph frame) enabled positioning of the recording electrodes exclusively at the infected sites. Scale bars, 1 mm.

EGFP and OMP in infected cells provided a mechanism to assess the heterogeneity in infectivity based on the observed green fluorescence. However, GFP fluorescence did not necessarily provide an accurate quantitation of OMP expression. Therefore, we did western blot analyses on extracts of olfactory epithelium from CMV-OMP-IRES-EGFP-AdV-infected OMP-null mice to obtain an estimate of the level of OMP expression. The OMP expressed *in vivo* after viral infection had the same electrophoretic mobility as recombinant OMP, and as the endogenous OMP synthesized in ORNs in control mice (**Fig. 1a**, lanes 1–7). As expected, no OMP was detected in the tissue from the OMP-null mice (**Fig. 1a**, lane 8). We used olfactory epithelia with visually estimated infection levels of 20–50% to prepare extracts for immunoblot analysis (**Fig. 1a**). The levels of OMP in extracts from an area with an estimated infection level of about 20% (**Fig. 1a**, lane 4) approximated that in tissue from control mice (**Fig. 1a**, lane 7). In highly infected areas of olfactory epithelium, as indicated by intense green fluorescence and an estimated infection rate of 50%, the level of OMP expression (**Fig. 1a**, lane 5) exceeded that in control mice (**Fig. 1a**, lane 7). Thus, although the extracts were derived from a mixture of both infected and uninfected cells, the band intensities indicated a high level of OMP expression due to the strong CMV promoter and the probability of multiple viral infections per cell. Although adenovirus preferentially infected olfactory neurons, it also infected sustentacular cells[11], which contributed to the intensity of the OMP band in the immunoblot analysis.

In addition to the analysis of OMP expression in total olfactory tissue, co-expression of OMP and EGFP by individual olfactory neurons of adult OMP-null mice infected with CMV-OMP-IRES-EGFP-AdV was determined. Coronal cryosections of the olfactory epithelium showed OMP expression, which was detected by immunohistochemistry using anti-OMP primary antibody and Cy3-labeled secondary antibody; EGFP was visualized directly (**Fig. 1b**). Olfactory neurons in the sections were identifiable by their typical morphology. The superimposed images of the antibody staining against OMP and GFP fluorescence (**Fig. 1b**, bottom) demonstrated that OMP and EGFP were co-expressed in infected olfactory neurons.

OMP expression affects response kinetics

The complex anatomy of the nasal cavity resulted in a variable extent of infection across the epithelium. This enabled selection of high and low areas of adenovirus-mediated OMP expression, in the same mouse, for electrophysiological analysis and comparison. Some regions exhibited a very high degree of infection (**Fig. 1c**, bottom), which were estimated to have more than 50% infected cells. More than 20% of the treated animals showed this high degree of infection, but due to the complex structure of the olfactory epithelium, the infected regions were not always in an

area well suited for electrophysiological recordings. Electrophysiological responses to odor stimulation were measured by electro-olfactogram (EOG) recordings and represented a sum of the electronegative generator potentials originating from many ORNs in the immediate (approximately 100 μm) proximity of the recording electrode. We measured EOG responses, at various sites, to three different odor concentrations and to three different odors in both OMP-null ($n = 8$) and control mice ($n = 8$). The odor stimuli used were amyl acetate, citralva and lilial, but the data show amyl acetate stimulation only, as similar results were obtained with all stimuli. To test the odor adaptation, we used a double-pulse protocol that included a conditioning pulse followed by a test pulse, separated by different time intervals (5, 10, 15 and 20 seconds). Our data (**Fig. 2**) confirmed and extended previous findings that the second response in OMP-null mice is significantly smaller and that overall, the response kinetics are slower in OMP-null mice. These results indicated that OMP participated in odor adaptation or recovery from adaptation.

The onset of the odor response was a rapid linear process that became a nonlinear function only near the peak of the response amplitude. The onset was best characterized by fitting the linear portion of the curve with a linear function ($y = k_1 + k_2t$; k_1, y-intercept; k_2, onset slope; t, time). Comparison of the curve fits showed that OMP-null mice had slower kinetics. Because the response kinetics depended on the amplitude, we normalized all calculated values by dividing them by the response amplitude (**Table 1**). The difference ($p < 0.001$) was most apparent at high odor concentrations (saturated vapors applied from the stimulus delivery tube containing a 1 mM odor solution). The actual concentration delivered to the tissue was significantly less than 1 mM because the stimulus was drawn from the headspace over the solution and further mixed with humidified air for delivery to the tissue. The responses elicited by odors at lower concentrations (0.1 mM odor solution) also exhibited significantly faster kinetics in both groups ($p < 0.05$). Differences for the lowest odor concentration (0.01 mM odor solution) were not statistically significant, probably because the responses were too small for reliable measurements.

The recovery curve of the odor response in both control and OMP-null mice was best characterized with a double-exponential function ($y = k_1 + k_2e^{-\tau 1t} + k_3e^{-\tau 2t}$; k_1, k_2 and k_3, constants; t, time; τ_1 and τ_2, time constants). A double-exponential function usually indicates two separate processes. In the case of EOG recordings, the two time constants could be ascribed to either cellular or population events. Within the same group (control or OMP-null), the difference between the two normalized time constants (slow, τ_1; fast, τ_2) increased as odor concentration was increased. Both the slow and fast time constants were 2–6-fold slower in OMP-null compared to control mice; this difference was also greater at higher odor concentrations (**Table 1**).

We did similar experiments on the OMP-null mice infected with CMV-OMP-IRES-EGFP-AdV ($n = 4$, multiple recording sites per mouse) using green fluorescence to select sites for recording. Because the OMP-null mice exhibited the strongest effect in response to high odor concentrations (1 mM in solution), we used the same concentration in OMP-null mice that were infected with the virus. To control for the influence of viral infection and EGFP expression on the EOG, adenovirus carrying the gene for EGFP but not OMP, driven by the CMV promoter, was used as a control. OMP-null mice infected with this virus did not show any rescue effect ($n = 7$, **Fig. 3a** and **b**).

Areas of high infection (more than 50% infection efficiency) showed fast onset (**Fig. 3a**) and recovery (**Fig. 3b**) kinetics, similar to those recorded in the control mice. Only responses recorded from these highly infected sites were used for kinetic analyses. We fitted the response onset with a linear function and the recovery curves with a double-exponential function. The fitted curves' time constants changed significantly, indicating rescue of the

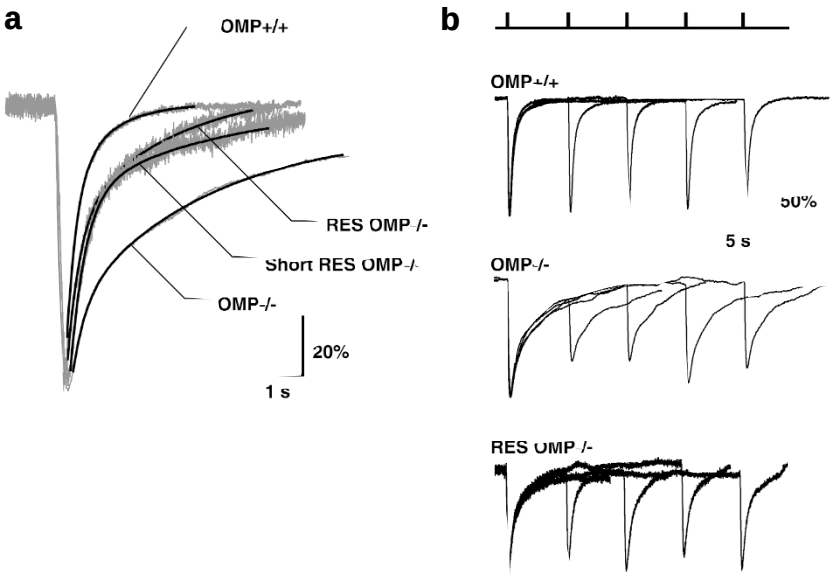

Fig. 2. Representative EOG traces from control, OMP-null and rescued OMP-null mice. (**a**) EOG recordings from the control (OMP +/+), OMP-null (OMP –/–) mice and OMP-null mice infected with OMP-adenovirus 3 days or 1 day after infection (RES OMP–/–, Short RES OMP–/–, respectively; actual traces are shown in gray). The recovery of the odor responses was fitted with double-exponential functions (shown in black). Traces were normalized to 100%, to allow easier comparison of time constants. (**b**) EOG recordings from the control (OMP +/+), OMP-null (OMP –/–) mice and OMP-null mice infected with CMV-OMP-IRES-EGFP-AdV (RES OMP–/–). Responses were obtained in a double-pulse protocol, where the first pulse was a conditioning pulse and the second (test) pulse was applied after a time interval of 5, 10, 15 or 20 seconds (as indicated by the small bars on the top of the EOG traces). In control mice, the second response almost completely recovered after 5 seconds. In the OMP-null mice, responses recovered much more slowly. In these mice, the second response started from a shifted baseline due to incomplete recovery of the first response, and its amplitude was much smaller than the amplitude of the first response. The size of the second response gradually increased with an increase in time interval. Bottom, traces represent EOG recordings from the OMP-null mice infected with CMV-OMP-IRES-EGFP-AdV, which exhibited responses with fast recovery; kinetics resembled responses in the control mice.

OMP-null phenotype. The normalized onset slope value (for 1 mM odor solution) was –7.30 ± 0.72 per second (compare this to values for control and OMP-null mice from **Table 1**); the normalized recovery time constants were 0.34 ± 0.05 per second per mV for the fast time constant (T_{r-1}) and 0.14 ± 0.03 per second per mV for the slow time constant (T_{r-2}). The onset rate in infected mice also seemed to be faster than in control mice, although this difference was not statistically significant.

To test whether the increase in OMP content above normal levels had an effect on response kinetics, we infected control mice with CMV-OMP-IRES-EGFP-AdV. Infected control mice showed a significant change ($p < 0.01$) in the onset kinetics (**Fig. 3a**; **Table 1**), whereas the time constants of the recovery curve did not show any significant increase (data not shown).

We also used the double-pulse protocol to assess the recovery of the odor response from adaptation. These experiments showed an increase of the ratio between the second (S) and first (F) responses in the infected OMP-null animals (S/F, **Fig. 3c**). The higher the S/F ratio, the better the recovery of the second response; a S/F ratio of 1.0 indicated a complete recovery from adaptation. Control mice had a similar average S/F ratio for all time intervals (ranging from 0.91 to 0.93; s.e.m., 0.01). Analysis of the average S/F ratio in OMP-null mice showed that for the 5-second interpulse interval, this ratio was much lower than in control mice (0.63 ± 0.02), and that it increased with an increase in the interpulse interval (0.77 ± 0.01 for the 10-second interval, 0.81 ± 0.01 for the 15-second interval and 0.84 ± 0.01 for the 20-second interval). In OMP-null mice infected with CMV-OMP-IRES-EGFP-AdV, there was an increase in the average S/F ratio. For the 5-second interpulse interval, the S/F ratio was 0.78 ± 0.02; for the 10-second interval, the ratio was 0.82 ± 0.02, for the 15-second interval, it was 0.84 ± 0.02, and for the 20-second interval, it was 0.92 ± 0.04. The increases in S/F ratio for the infected mice were statistically significant for the 5-second and 10-second interpulse intervals ($p < 0.05$), but not for the 15-second and 20-second intervals. (There was a large variability in calculated S/F ratios in infected mice due to different degrees of infection.)

EOG of cell number versus cell content of OMP

The varying intensity of EGFP expression (as an indicator of OMP expression) across the infected olfactory epithelia demonstrated that the efficacy of AdV infection was heterogeneous. Therefore, assuming that the adenovirus infected ORNs at random, we anticipated that a site with a lower infection rate would exhibit a smaller degree of rescue, independent of test odor. EOG recordings from the infected sites showed variable degrees of rescue (**Fig. 4a**) that correlated with the extent of infection, as estimated visually from the intensity of EGFP fluorescence. This effect was the same for all odors tested (data not shown). To control for variation in the responses from different turbinates or zones, we compared the responses in infected mice to the responses recorded from the same sites in their uninfected siblings (**Fig. 4b**), as estimated by the distance from the edges of the turbinate and from the respiratory epithelial boundary.

Table 1. Statistical analyses of odor responses.

	Animal condition		Odor concentration		
			Low	Medium	High
Onset slope (normalized, per s)	Control		–7.77 ± 0.40	–6.78 ± 0.33	–6.37 ± 0.28
	OMP-null		–6.61 ± 0.86	–5.08 ± 0.65	–4.42 ± 0.25
	t-test (C versus KO)		NS	$p < 0.05$	$p < 0.001$
	Rescue		ND	ND	–7.30 ± 0.72
	t-test (R versus KO)		ND	ND	$p < 0.001$
	Overexpressed		ND	ND	–7.66 ± 0.29
	t-test (OC versus C)		ND	ND	$p < 0.01$
	Control for virus		ND	ND	–4.21 ± 0.32
	Heterozygotes		–8.23 ± 0.27	–7.30 ± 0.22	–6.44 ± 0.29
Recovery kinetics (normalized T per s, per mV)	Control	**T1**	0.48 ± 0.10	0.37 ± 0.07	0.26 ± 0.08
		T2	0.45 ± 0.09	0.33 ± 0.06	0.13 ± 0.03
	OMP-null	**T1**	2.12 ± 0.58	2.05 ± 0.63	1.63 ± 0.30
		T2	0.78 ± 0.12	0.61 ± 0.11	0.57 ± 0.16
	t-test (C versus KO)	**T1**	NS	$p < 0.05$	$p < 0.05$
		T2	NS	$p < 0.05$	$p < 0.05$
	Rescue	**T1**	ND	ND	0.34 ± 0.05
		T2	ND	ND	0.14 ± 0.03
	t-test (KO versus R)	**T1**	ND	ND	$p < 0.05$
		T2	ND	ND	$p < 0.05$
	Control for virus	**T1**	ND	ND	1.86 ± 0.35
		T2	ND	ND	0.60 ± 0.09
	Heterozygotes	**T1**	0.51 ± 0.08	0.36 ± 0.07	0.25 ± 0.10
		T2	0.46 ± 0.10	0.32 ± 0.06	0.14 ± 0.03

Onset slope and recovery curves of the odor response were fitted with linear and double exponential curves, respectively. Time constants were normalized by dividing their values with the response amplitude (T). C, control ($n = 8$); KO, OMP-null animals ($n = 8$); R, OMP-null animals infected with CMV-OMP-IRES-EGFP-AdV ($n = 4$); OC, control animals infected with CMV-OMP-IRES-EGFP-AdV ($n = 2$); control for virus, OMP-null mice infected with a control virus ($n = 7$). Low, medium and high odor concentrations applied as saturated vapors above 10^{-5}, 10^{-4} and 10^{-3} M odor solutions in stimulus delivery tube, respectively. Data are presented as average ± standard error. NS, not significant; ND, not determined.

The dependence of the extent of EOG rescue on relative levels of OMP expression could result from the amount of OMP expressed in each individual olfactory neuron, from the number of neurons infected or a combination of the two. The availability of control, heterozygous and homozygous OMP-null mice provided an opportunity to test the effect of OMP dosage on the EOG responses to odor stimuli. Our previous immunoassay data[6] indicated that heterozygous OMP-null mice expressed 40–50% less OMP than littermate control mice. To determine whether this difference in OMP expression reflected a reduction in numbers of OMP-expressing ORNs or a reduction in OMP content per ORN. We evaluated OMP expression by immunocytochemistry in coronal sections of null, heterozygous and control mice (**Fig. 4c**). The distribution of OMP immunoreactive ORNs seemed to be identical between control and heterozygous mice. This observation, along with previous immunoassay results[6], indicated a reduced content of OMP in all ORNs of the heterozygote, rather than a full complement of OMP in one half and no OMP in the other half of the ORNs. Odor responses recorded from heterozygous mice ($n = 2$, multiple recording sites per mouse) exhibited kinetics similar to those seen in control mice (**Fig. 4c**, insets), indicating that the reduced level of OMP expression in the olfactory neurons of heterozygous mice was still sufficient to maintain normal physiological responses. Normalized values for responses to three odor concentrations were not different from control values (**Table 1**). These data further suggested that the dose effect observed with different infection levels reflects the variable number of infected cells.

Discussion

Viral rescue of OMP-null phenotype

Studies of OMP-null mice generated by homologous recombination demonstrate both electrophysiological and behavioral deficits in olfactory function[6,7]. Here we show that the OMP-null electrophysiological phenotype is due to the absence of OMP and its role in the overall transduction process. We delivered the OMP gene to adult OMP-null mice *in vivo* and demonstrated that short-term expression restored normal olfactory function. EOG responses recorded from the olfactory neuroepithelium of OMP-null mice infected with CMV-OMP-IRES-EGFP-AdV were virtually identical to those of control mice, within three to four days after infection. Although we cannot completely rule out the possibility that OMP is involved in some structural or developmental events, it is likely that OMP is directly involved in the signal transduction pathway, and does not exert its primary effect through structural alterations in the cell. Several additional observations were consistent with this view. First, our use of adult mice precluded the involvement of developmental events. Second, the histology and immunocytochemistry for carnosine in mature ORNs, the density of dendritic knobs on the surface and GAP43 immunostaining of immature ORNs are the same in control and OMP-null mice[6]. Third, BrdU uptake was essentially the same in control and OMP-null mice (D.M. Cummings and F.L.M., unpublished observations. Fourth, there is no alteration in olfactory axon conductance velocity[14] indicating no major change in other electrical properties of ORNs in OMP-null versus control mice.

Moreover, the EOG responses recorded from sites with different degrees of OMP expression showed proportional magnitudes of rescue. Because the EOG represents a measurement of activity from a population of neurons, each data point derived from a mixture of two types of neurons (rescued and OMP-null neurons), which independently contributed to the summed EOG responses. Thus, the faster kinetics measured in EOG responses from the infected mice could be attributed to either much faster kinetics of the infected ORNs (due to much higher expression of OMP driven by the strong CMV promoter) or solely to the total number of infected neurons contained within the recording site and not affected by OMP overexpression. To further examine the influence of OMP expression on the EOG, we obtained recordings from heterozygous OMP-null mice, in which each ORN contained a lower amount of OMP than that present

Fig. 3. Summary of EOG data showing onset and recovery kinetics of odor responses and the recovery from adaptation in control, OMP-null and adenovirus-infected mice. (**a**) Onset slope normalized by dividing its value with the response amplitude. (**b**) Normalized time constants of the recovery phase of the response. T_{ctrl}, time constants in control mice, T_{KO}, time constants from OMP-null mice, T_r, time constants from OMP-null mice infected with CMV-OMP-IRES-EGFP-AdV, T_{gfp}, time constants from OMP-null mice infected with adenovirus containing EGFP but not OMP. Asterisk indicates statistically significant increase in time constants in infected mice compared to OMP-null animals. For T_{r-1}, $p < 0.001$; for T_{r-2}, $p < 0.05$. (**c**) The effect of CMV-OMP-IRES-EGFP-AdV infection on adaptation, as measured by double-pulse protocol. Values are represented as a ratio between the second and first response (S/F) at different time intervals (bottom axis). Asterisk indicates statistically significant recovery in S/F ratio in infected animals compared to OMP-null mice ($p < 0.05$).

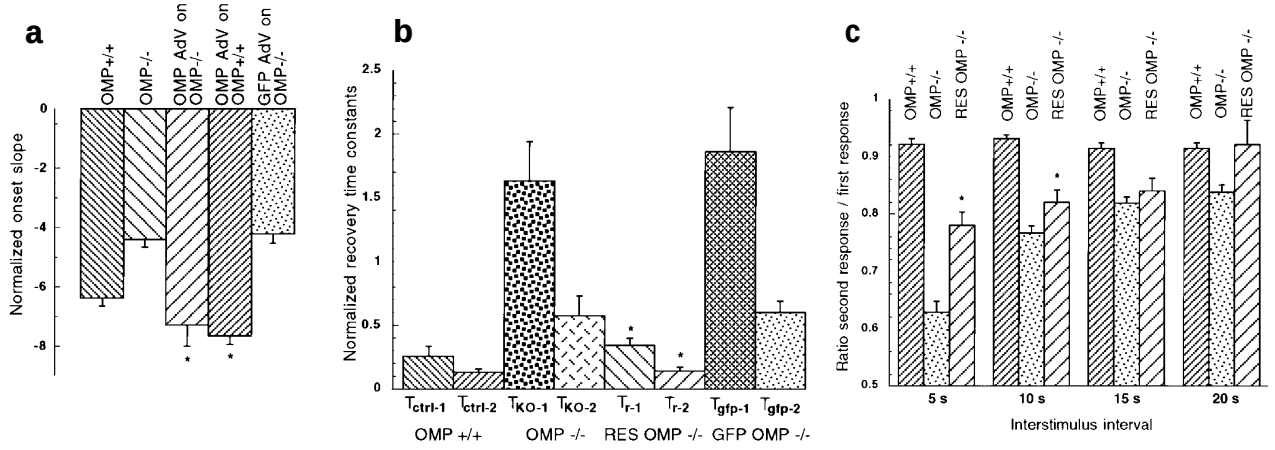

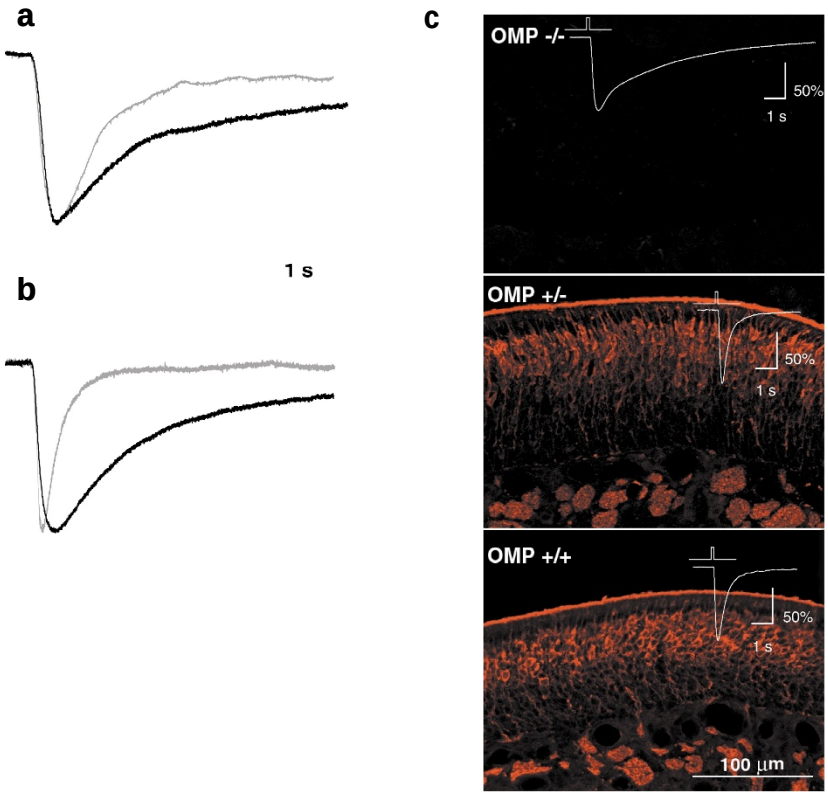

Fig. 4. The effect of infection rate and OMP levels on EOG responses. (**a**) Different degrees of infection (gray, more infected area; black, much less infected area) with CMV-OMP-IRES-EGFP-AdV in the same mouse resulted in different onset and recovery kinetics. (**b**) EOG response recorded from highly infected area in one animal (gray) compared to response recorded from the same spot in its uninfected sibling (black). (**c**) Immunocytochemistry demonstrated that there is no OMP expression in OMP-null (OMP –/–) mice and demonstrated a lower level of OMP expression in heterozygous (OMP +/–) mice compared to control (OMP +/+) mice. Insets, representative EOG traces from OMP-null, heterozygous and control mice.

in ORNs of control mice. The EOGs obtained were identical in heterozygous and control mice. These data demonstrated that a population of ORNs with reduced cellular contents of OMP could still maintain normal response kinetics.

To test whether response kinetics could be further increased in the control adult mice, we infected them with CMV-OMP-IRES-EGFP-AdV. EOG recordings indicated that overexpression of OMP in control mice increased the onset rate but not the recovery kinetics. Thus, although normal response kinetics did not require that OMP levels be as high as those found in the control tissue, it seemed that further rise of the endogenous OMP concentration in the mature ORNs of control (OMP +/+) mice further increased the initial rapid response rate.

Analysis of paired-pulse experiments demonstrated that, in addition to restoring the response kinetics, OMP reversed the reduced magnitude of the second response. The ratio between the second and the first response for the 5-second interstimulus interval in the mice treated with AdV was in the range of 0.7–0.87. This range was close to the values of 0.84–1.07 found in control mice but differs greatly from the range of 0.42–0.73 observed in the OMP-null mice, demonstrating an increase in the S/F ratio for the CMV-OMP-IRES-EGFP-AdV infected mice. This effect also correlated with the level of OMP expression, as EOGs from infected mice that showed larger improvements in response kinetics also manifested a higher ratio between the second and first response. Taken together, these data demonstrated rescue of the OMP-null phenotype by CMV-OMP-IRES-EGFP-AdV infection.

A possible function of OMP

The analysis of individual EOG responses demonstrated that OMP was involved in regulating the response kinetics after odor stimulation. The EOG kinetics in OMP-null mice were slower for both the onset and termination of the odor-induced responses and exhibited an impaired ability to respond to the second stimulus in paired-pulse experiments. These two phenomena—the slowed kinetics and reduction in response to the second pulse—could be either causally related or independent. However, the results we obtained following infection with CMV-OMP-IRES-EGFP-AdV demonstrated that both effects were dependent on OMP, as both are restored in the CMV-OMP-IRES-EGFP-AdV infected OMP-null mice. What common mechanism might account for this dependence? The onset kinetics reflect kinetics of processes involved in activation of the signal transduction pathway, such as activation of first the odor receptor, then the G-protein, then adenylate cyclase, followed by production of cAMP and the activation of the cAMP-gated channels involved in the formation of the generator potential. On the other hand, the recovery kinetics reflect channel-closing and possibly the increase in the phosphodiesterase activity, with subsequent decreased cAMP levels and elimination of the Ca^{2+} that enters through the cAMP-gated channels. Both onset and recovery kinetics reflect dynamic changes in ion channels involved in the signal transduction pathway. Therefore, we propose that OMP regulates the sensitivity of one of the channels involved in the transduction process. Detailed electrophysiological analysis of the odor responses at the single-cell level will identify OMP's site of action.

Additional participants, which may be at checkpoints modulated by OMP, may influence the olfactory signal transduction pathway. For example, single-channel recordings suggest the existence of two populations of CNG channels with different pharmacological properties in the sensory membrane of ORNs[15,16]. In addition, cytoplasmic calcium and calmodulin decrease cAMP sensitivity[17]. The mechanisms of these processes are not fully known. Other undetermined endogenous factors may mediate these effects and may also be candidates for OMP modulation.

In summary, we have used a recombinant adenovirus to restore OMP expression *in vivo* in adult OMP-null mice. This intervention has rescued the OMP-null phenotype and is consistent with the hypothesis that OMP is involved in the olfactory signal transduction pathway. These experiments have restricted the possible functions of OMP; further studies may determine the precise mechanism of OMP action in olfactory transduction.

Finally, our results demonstrate successful *in vivo* gene deliv-

ery, phenotypic rescue of a targeted gene deletion, and restoration of deleted gene product function in the adult vertebrate olfactory system. Our results have implications for the study of short-term effects of induced somatic gene expression to rescue deleted genes, and the study of effects of ectopic gene expression.

Methods

All experiments followed NIH guidelines and were done in full compliance with the Columbia University Institutional Animal Care and Use Committee.

Adenoviral constructs. The recombinant adenoviral construct used was generated as described previously[18]. This procedure depends upon homologous recombination between the E1–E3 deficient replication-defective adenovirus type 5 (Ψ5) and the shuttle vector pAdlox. The expression cassette in pAdlox, governed by the cytomegalovirus promoter (CMV) and the simian virus 40 (SV40) polyadenylation signal, is inserted between the virus packaging site (Ψ) and the recombination signal sequence (loxP). The expression unit is incorporated into new viruses in a cre-recombinase-mediated process after transfection of both constructs into CRE8 cells that constitutively express crerecombinase. The resulting recombinant viruses have a single loxP site and thus outgrow the Ψ5 virus (two loxP sites) through negative selection in the presence of crerecombinase.

Generation of the expression cassette in pAdlox. The bicistronic expression cassette, consisting of the coding region for the mouse olfactory marker protein[6], followed by an internal ribosome entry site (IRES)[19] and the coding region for the enhanced green fluorescent protein (EGFP, Promega, Madison, Wisconsin), was generated as follows. A fragment containing the entire coding region of the OMP gene was obtained by a standard PCR protocol using a mouse genomic OMP subclone as template. To facilitate subsequent cloning procedures, upstream and downstream PCR primers were designed to introduce a *Hin*dIII and an *Eco*RI recognition site at the 5′ and 3′ ends of OMP, respectively. The 516 bp *Hin*dIII-*Eco*RI digested PCR fragment of OMP and a 1.25 kbp EcoRI-XbaI restriction fragment carrying the IRES-EGFP sequence (clone pBSK-IRES-EGFP) were cloned into the *Eco*RI-*Xba*I linearized shuttle vector pAdlox. The OMP sequence in pAdlox was verified by sequencing.

Viral generation and purification. Recombinant adenovirus (CMV-OMP-IRES-EGFP-AdV) was generated by homologous recombination. Ψ5 viral DNA (1 μg) and pAdlox-OMP-IRES-EGFP (1.8 μg, *Sfi*I digested) were cotransfected into an 80% confluent monolayer of CRE8 cells according to a standard procedure (Lipofectamine, Gibco-BRL, Rockville, Maryland). After six hours, the transfection mixture was replaced with DMEM (Dulbecco modified Eagle medium, high glucose, GIBCO-BRL) supplemented with 10% FCS (fetal calf serum, JRH Biosciences, Shawnee Mission, Kansas), and cells were maintained and fed until the cell lysis was complete (5 days). For virus plaque purification, a 1:300 dilution of the cell lysate in DMEM was used to infect HEK 293 monolayer cells (ATCC, Manassas, Virginia). After 4 hours the virus solution was removed, and the cells were overlaid with 0.8% Noble-agar (Difco Laboratories, Detroit, Michigan) in MEM (Gibco-BRL), supplemented with 10% FCS and 12 mM $MgCl_2$ and maintained until the presence of recombinant viral plaques was visualized under an inverted microscope (Nikon Diaphot, FITC filter). Individual plaques were selected and subjected to two additional rounds of plaque purification. A large-scale preparation of recombinant virus from a single plaque was propagated in HEK 293 cells and purified through cesium chloride gradient centrifugation; the viral titer (1.3×10^{10} plaque forming units per ml) was determined by plaque assay. The monocistronic viral construct CMV-EGFP-AdV that was used in control experiments carries the coding region of the green fluorescent protein (S65T mutant) only[20].

Western blot analysis of OMP expression in HEK 293 cells. The proper expression of OMP was verified by western blot analysis. A subconfluent monolayer of HEK 293 cells was infected with CMV-OMP-IRES-EGFP-AdV virus. Two days after infection, cells were collected, washed and ruptured by several freeze-thaw cycles, and cellular debris was removed by centrifugation. Aliquots of the lysate and recombinant OMP and cytosolic extracts of mouse olfactory tissue were subjected to SDS-PAGE under reducing conditions, electrophoretic transfer to a PVDF membrane (Millipore, Bedford, Massachusetts) and immunoblot analysis for OMP (primary rabbit-anti-OMP 1:50000, secondary peroxidase-conjugated goat anti-rabbit, 1:40000, Sigma, St. Louis, Missouri) using a standard procedure. OMP immunoreactivity was visualized using an enhanced chemiluminescence system according to the manufacturer's recommendations (ECL-Plus, Amersham Pharmacia Biotech, Piscataway, New Jersey). Signal detection and analysis was done on a STORM Imager with ImageQuant (Molecular Dynamics, Sunnyvale, California).

Viral infections. Adult mice were anesthetized (ketamine, 90 mg per kg and xylazine, 10 mg per kg) and the epithelium of the right nostril was infected with 5 μl of the viral stock solution (1.3×10^{10} plaque forming units per ml) diluted 1:4 (v/v) with PBS (total volume 20 μl). The viral solution was delivered through PE10 tubing with a Harvard pump (Harvard Apparatus, Holliston, Massachusetts), injecting at the rate of 4 μl/min. Our previous experience in infecting rat olfactory epithelium using adenovirus[12] indicated an infection efficiency of about 10–20%, which we anticipated would not be sufficient to unequivocally observe the rescue of the OMP-null phenotype. To increase the infection rate, we re-infected each mouse on three consecutive days.

Immunohistochemistry for OMP and GFP. Three days after infection (CMV-OMP-IRES-EGFP-AdV) OMP-KO mice were anesthetized as above and transcardially perfused with ice-cold Pipes buffer (0.1 M Pipes, 2 mM $MgCl_2$, 5 mM EGTA, pH 6.9) followed by 4% paraformaldehyde in Pipes buffer. Mice were decapitated, their heads collected, trimmed and cryoprotected in 30% sucrose overnight at 4°C. The tissue was embedded in OCT (Tissue Tek, Sakura, Torrance, California) and snap-frozen in a dry ice/acetone bath. Fifteen-micron coronal cryosections of the olfactory epithelium were cut, thaw-mounted onto slides (Superfrost Plus, Fisher Scientific, Hanover Park, Illinois) and treated with a preincubation solution of 0.1% Triton X-100 and 4% normal horse serum (Vector Laboratories, Burlingame, California) in PBS for 1 hour at room temperature. Immunohistochemistry for OMP was done using primary goat anti-OMP antibody (1:5000 in preincubation solution overnight at 4°C) and cy3-conjugated secondary anti-goat antibody (1:800 in preincubation solution, 1 hour at room temperature). Separate control reactions done by omitting either the primary or secondary antibody did not exhibit any immunoreactivity. Sections were rinsed in PBS after each antibody application, coverslipped using fluorescent mounting medium (DAKO, Carpinteria, California) and visualized by confocal microscopy (Olympus Fluoview, BX50WI, Olympus America, Melville, New York) with appropriate excitation and emission barrier filters. GFP was visualized directly. For each of the fluorescent images shown, a series of 2 μm optical sections was acquired and combined by Fluoview 1.1.

EOG recordings. Three to four days after infection (in one case, one day after infection), mice were overdosed with anesthetics and decapitated. We observed a very high infection rate within the infected regions, more than 50% of the cells. Green fluorescence, indicating expression of EGFP, allowed us to position the recording electrodes either at the highly infected sites or at uninfected sites in the same mouse. The application of the odor stimuli and EOG recordings were done as described earlier[12]. In brief, the odor stimulus (citralva, lilial or amyl acetate) was delivered by a 100-ms long pressure pulse of air that displaced the saturated odor vapor in the head space from the tube containing odor solution (0.01, 0.1 or 1 mM) into the steam of humidified clean air through the delivery tubing onto the olfactory epithelium. Our estimate, based on the immersed EOG recordings where odor concentration could be controlled (unpublished observation) was that final odor concentration reaching the olfactory epithelium would be at least an order of magnitude smaller than the concentration of an odor solution in the test tube. Responses were amplified by a DP-301 differential amplifier (Warner Instrument, Hamden, Connecticut) and acquired by Power Macintosh G3. Stimulus pulse delivery and data acquisition was controlled with the Igor Pro program (WaveMetrics, Lake Oswego, Oregon).

Data analysis. Response curves were fitted by the Igor Pro program. Values in the text and figures are expressed as average ± standard error. Statistical significance between two groups was evaluated with two-tailed *t*-test for independent samples. Probability values of less than 0.05 were considered statistically significant.

Acknowledgements

We thank P. Mombaerts for providing the pBSK-IRES-EGFP clone, S. Hardy for providing shuttle vector pAdlox and CRE8 cell line and K. Moriyoshi for providing CMV-EGFP-AdV. We thank Matthew Rogers and Dong-Jing Zou for suggestions on the manuscript. This research was supported by NIH grant DC R01-03112 (F.L.M.).

Received 24 May; Accepted 8 September 2000

1. Margolis, F. L. A brain protein unique to the olfactory bulb. *Proc. Natl. Acad. Sci. USA* **69**, 1221–1224 (1972).
2. Keller, A. & Margolis, F. L. Isolation and characterization of rat olfactory marker protein. *J. Biol. Chem.* **251**, 6232–6237 (1976).
3. Krishna, N. S. R., Getchell, T. V., Margolis, F. L. & Getchell, M. L. Amphibian olfactory receptor neurons express olfactory marker protein. *Brain Res.* **593**, 295–298 (1992).
4. Buiakova, O. I., Krishna, N. S. R., Getchell, T. V. & Margolis, F. L. Human and rodent OMP genes: conservation of structural and regulatory motifs and cellular localization. *Genomics* **20**, 452–462 (1994).
5. Sydor, W. *et al.* Amino acid sequence of a unique neuronal protein: rat olfactory marker protein. *Arch. Biochem. Biophys.* **249**, 351–362 (1986).
6. Buiakova, O. I. *et al.* Olfactory marker protein (OMP) gene deletion causes altered physiological activity of olfactory sensory neurons. *Proc. Natl. Acad. Sci. USA* **93**, 9858–9863 (1996).
7. Youngentob, S. L. & Margolis, F. L. OMP gene deletion causes an elevation in behavioral threshold sensitivity. *Neuroreport* **10**, 15–19 (1999).
8. Farbman, A. I., Buchholz, J. A., Walters, E. & Margolis, F. L. Does olfactory marker protein participate in olfactory neurogenesis? *Ann. NY Acad. Sci.* **855**, 248–251 (1998).
9. Horwitz, M. S. in *Virology* (eds. Fields, B. N. & Knipe, D. L.) 1679–1721 (Raven Press, New York, 1990).
10. Zhao, H., Otaki, J. M. & Firestein, S. Adenovirus-mediated gene transfer in olfactory neurons *in vivo*. *J. Neurobiol.* **30**, 521–530 (1996).
11. Holtmaat, A. J. *et al.* Efficient adenoviral vector-directed expression of a foreign gene to neurons and sustentacular cells in the mouse olfactory neuroepithelium. *Mol. Brain. Res.* **41**, 148–156 (1996).
12. Zhao, H. *et al.* Functional expression of a mammalian odorant receptor. *Science* **279**, 327–242 (1998).
13. Touhara, K. *et al.* Functional identification and reconstitution of an odorant receptor in single olfactory neurons. *Proc. Natl. Acad. Sci. USA* **96**, 4040–4045 (1999).
14. Griff, E. R., Greer, C. A., Margolis, F., Ennis, M. & Shipley, M. T. Ultrastructural characteristics and conduction velocity of olfactory receptor neuron axons in the olfactory marker protein-null mouse. *Brain Res.* **866**, 227–236 (2000).
15. Frings, S. & Lindemann, B. Current recording from sensory cilia of olfactory receptor cells in situ. I. The neuronal response to cyclic nucleotides. *J. Gen. Physiol.* **97**, 1–16 (1991).
16. Nakamura, T. & Gold, G. H. A cyclic-nucleotide gated conductance in olfactory receptor cilia. *Nature* **325**, 442–444 (1987).
17. Kleene, S. J. Both external and internal calcium reduce the sensitivity of the olfactory cyclic-nucleotide-gated channel to cAMP. *J. Neurophysiol.* **81**, 2675–2682 (1999).
18. Hardy, S., Kitamura, M., Harris-Stansil, T., Dai, Y. & Phipps, M. L. Construction of adenovirus vectors through Cre-lox recombination. *J. Virology* **71**, 1842–1849 (1997).
19. Kim, D. G., Kang, H. M., Jang, S. K. & Shin, H. S. Construction of a bifunctional mRNA in the mouse by using the internal ribosomal entry site of the Encephalomyocarditis virus. *Mol. Cell. Biol.* **12**, 3636–3643 (1992).
20. Moriyoshi, K., Richards, L. J., Akazawa, C., O'Leary, D. D. M. & Nakanishi, S. Labeling neural cells using adenovirus gene transfer of membrane-targeted GFP. *Neuron* **16**, 255–260 (1996).